IEEE TRANSACTIONS ON
INDUSTRY
APPLICATIONS
A PUBLICATION OF THE IEEE INDUSTRY APPLICATIONS SOCIETY
WWW.IEEE.ORG/IAS
SERVING OUR MEMBERS AND SUBSCRIBERS IN OUR FIFTY-THIRD YEAR OF PUBLICATION

A Quadratic Programming Based Optimal Power and Battery Dispatch for Grid Connected Micro Grid

Tim G. Paul, *Student Member, IEEE,* Sheikh J. Hossain, *Student Member, IEEE,* Sudipta Ghosh, *Member, IEEE,* Paras Mandal, *Senior Member, IEEE,* and Sukumar Kamalasadan, *Senior Member, IEEE*

***Abstract*—In this paper, the concept of end-user driven micro grid is introduced and an economic dispatch framework is proposed for optimal power and battery scheduling of such a micro grid. The main advantage is that unlike other centralized approaches reported in the literature, the proposed architecture provides end-user flexibility, optimally manages the battery minimizing the power required from the grid and at the same time ensures grid level reliability. The proposed optimal scheduling is first validated on a grid connected micro grid including a photovoltaic (PV) farm and a battery, considering the grid as a dispatchable power source. Then the architecture is compared with one of the existing centralized optimization approaches. To demonstrate the applicability and scalability, the architecture is further evaluated on a modified IEEE 33 bus distribution feeder including multiple micro grids suitable for real-time implementation. The test results indicate that the approach is optimal, scalable, feasible, improves feeder reliability, and provides maximum utilization of the PV arrays.**

***Index Terms*—Battery power dispatch, economic dispatch, grid connected end-user driven micro grid, optimal scheduling, quadratic programming.**

NOMENCLATURE

N	Total number of samples
t	Time instant
$E(t)$	Instantaneous energy of the battery
dt	Time interval
$P_{batt}(t)$	Instantaneous battery dispatch value.
P_{batt}^{min}	Minimum power rating of the battery
P_{batt}^{max}	Maximum power rating of the battery
$P_{load}(t)$	Total load at instant t
$P_{pv}(t)$	Photovoltaic generation at instant t
$P_{grid}(t)$	Power demand from the Electric grid
P_{grid}^{min}	Minimum power demand from the Electric grid
P_{grid}^{max}	Maximum power demand from the Electric grid
$P_2(t)$	Total power from PV plus the battery
SOC	State of charge at the Battery
MG	Micro grid
A_{eq}	Coefficient matrix of equality constraints
A	Coefficient matrix of inequality constraints
b_{eq}	Vector for constant coefficients
b	Vector for constant coefficients of inequality constraints
H	Symmetric matrix describing the coefficients of the quadratic terms
C	Vector of linear terms
l	Vector of lower bound of variables
u	Vector of upper bound of variables
x	Solution vector

This work was supported in part by the Energy Production Infrastructure Center (EPIC) and National Science Foundation under the grant NSF Grant ECS- 1309911. T. G. Paul, S. J. Hossain, S. Ghosh and S. Kamalasadan are with the EPIC and Department of Electrical and Computer Engineering, University of North Carolina at Charlotte, Charlotte, NC 28223 USA. P. Mandal is with the Department of Electrical and Computer Engineering, University of Texas at El Paso, TX 79968 USA.

Digital Object Identifier 10.1109/TIA.2017.2782671

I. INTRODUCTION

IN order to satisfy the increased electricity demand and global environmental regulations, recently there is a move towards realizing a non fossil fuel based power grid. Grid connected renewable power systems have gained great interest in this respect. One of the main renewable energy based energy resources is PV systems. As opposed to wind farms that are mainly controlled and regulated by the utility, PV farms are distributed across the regulated and non-regulated business. A major challenge for PV generation is in managing the intermittent energy production with varying power demand. On the source side, one way of mitigating this intermittency is to provide additional energy storage system (ESS) to the PV farm. This is mainly provided using battery energy storage system (BESS). Especially in the power distribution set up, such a discrete energy system consisting of distributed energy resources including storage, generation and load management can be developed, namely micro grid. A micro grid can operate in parallel with another micro grid as well as independently from the main grid or connected to the grid. Several approaches have been proposed for energy management and control of micro grid with renewable sources and storage especially with PV [1], [2]. Most of such previous approaches discussed regulated (controlled by the utility) management of micro grids.

As opposed to utility driven micro grids, end-user driven micro grids are managed by the end-users. Such micro grids normally exist at the low voltage end of the power distribution feeder (either at 120V or at 480V level) and connected to the utility through inverters. Normally these systems are seen as roof-tops or community level installations. Such micro grids can provide higher reliability, optimal active power balance (a mechanism in which the local power is utilized to the maximum and at the same time grid constraints are satisfied) and enhance customer participation. However, the main challenges of such installations are a) the visibility issue related to the power usage as these installations are mostly behind the meter (BTM) and b) the issues related to the usage of the electricity based on the need and comfort of the end-user versus economic and reliable operation of the utility.

Thus, a coordinating energy management architecture that considers the end-user need and economic and reliable operation of the grid is essential [3]–[7]. The coordination feature is mainly to achieve an integrated decentralized and centralized dispatch inspite of the respective modes of operation of the micro grid. Such micro grid energy management systems (EMS) should minimize the operation costs considering the reliability of the grid, and at the same time, allow end-user flexibilities such as using the micro grid energy resources based on the end-user needs. An economic dispatch approach can perform optimal power and battery scheduling considering utility side and end-user side objectives. Utility side applications could focus on optimizing properties of micro grid output for distribution upgrade deferral which means delaying the utility investments in distribution system upgrades, transmission support, and others, while the end-user side's objective is to maintain the demand flexibility.

Most of the earlier work related to micro grid management considered battery constraints to complete a centralized grid power flow optimization problem [8]–[10] such that it benefits the utility. Such centralized model collects all the necessary information for micro grid scheduling and performs centralized operation and control. The main drawbacks of the centralized scheme are reduced flexibility for the end-user and in adding new components, and extensive computational requirements. For example, if a new energy resource (device) is added to the grid or is out for maintenance then the EMS operation is interrupted to add/remove device specific constraints from the algorithm that implements the EMS. Further, any change of a particular unit dispatch would require a new optimal power flow to be run for the system, because they are all integrated in a single optimization problem. In addition, the dynamic nature of energy storage dispatch creates time domain couplings among all decision variables as well as stochastic variables like loads and renewable power. This poses challenges for the computational complexity of centralized formulation.

The issues with centralized formulation can be avoided with decentralized or distributed formulations. In the distributed scheme each component of the micro grid is considered separate and makes its own decisions. The optimal schedule is obtained by iterative data transfers among the components. Since the micro grid is integrated with storage it makes the optimization problem dynamic, i.e., it is time dependent. Different optimization techniques have been used to formulate this type of dynamic scheduling problem [8], [11]–[19]. References [12]–[16], [20], [21] used dynamic programming to solve the dispatch problem. References [22], [23] proposed model predictive control (MPC) based controller to control the output of BESS which is used in micro grid management. In [24], a distributed EMS is implemented based on alternating direction method of multipliers (ADMM) where dispatch information is passed between generators and BESS with a goal to meet the total demand. In [25], a distributed formulation of the economic dispatch is shown where the goal is to maximize the profit for each energy resource. The main issues with distributed framework is that maximum benefits for the utility are not always satisfied and it is also difficult to maintain grid level stability.

In our previous work [26], we proposed a dynamic optimization approach that reduces the grid operational cost, and at the same time, maximizes the PV output power based on optimal scheduling of the battery. This paper is an expanded version of [26] where the the proposed quadratic programming based optimal power scheduling approach is enhanced to provide optimal dispatch of the battery that enables grid reliability, economic dispatch and end-user flexibilites. The evaluation is done on utility scale real-life grid models.

The main advantages of the proposed approach are:

- The methodology provides economic dispatch by only using the micro grid tertiary control for calculating the active power set points such that the micro grid uses minimum power from the grid and the battery dispatch is optimized based on short-term PV generation data.
- The method works effectively with multiple micro grids and the grid reliability is maintained.
- The approach is scalable and can be implemented in real systems interconnected with power distribution grid.
- The approach provides end-user flexibility and at the same time ensures grid requirements.

The paper is organized as follows. In section II theoretical framework and problem formulation is discussed. This includes the fixed and predictive horizon methodologies. In section III simulation results for the proof-of-concept and integrated multiple micro grids connected to a distribution feeder are presented. Section IV concludes the work.

II. Economic scheduling of end-user driven micro grid

Conventional framework for a grid connected micro grid economic dispatch problem can be found in [27]–[32]. In such framework a centralized economic dispatch optimization is performed integrating micro grid devices such as BESS and renewable energy resources. In this paper, the concept of end-user driven micro grid is introduced for the first time. Then, an optimization framework is proposed to satisfy user-defined load (flexibility), maximizing the renewable energy based power extraction and at the same time ensuring minimum power import from the grid while honoring grid reliability. In this section, we will first define the end-user driven micro grid, and provide the proposed dynamic economic dispatch optimization framework including the formulation of the objective function and constraints. Further, we will discuss the adaptivity of the method to fulfill end-user and utility requirements and show the closed-loop implementation flowchart.

A. Customer-driven Micro Grid and End-user Driven Micro Grid

Electric power micro grids have been broadly classified as utility micro grids, industrial/commercial micro grids and remote/residential micro grids [5]. In recent years, a new paradigm of micro grids is being introduced to bring near real time information and control at the customer end. This type of micro grids is termed as customer-driven micro grid [5]. A customer-driven micro grid is a type of micro grid which can import or export real and reactive power when operated in grid connected mode and can also operate in islanded mode [4]. The

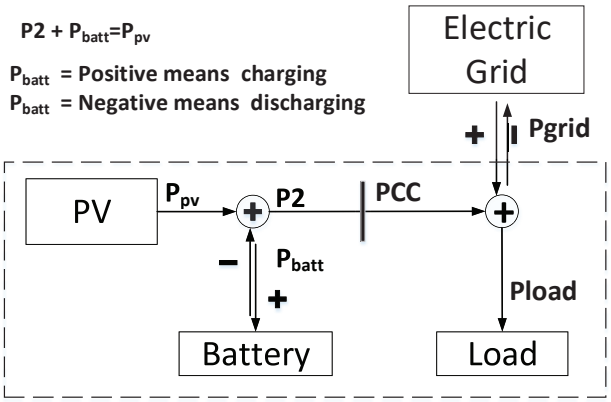

Fig. 1. Grid architecture for dynamic dispatch.

customer-driven micro grid provides a complete framework for the design, operation and economics of the micro grids from the customer standpoint. In this paper, the concept of end-user driven micro grid is introduced. The characteristics of end-user driven micro grid are: a) end-user should be able to drive, control and manage the micro grid, b) end-user driven micro grid should be able to sell power to the utility, c) it should be able to share active or reactive power with the utility grid, and d) it should be able to work in islanded mode. The main difference between a customer-driven and end-user driven micro grid is that in the former type, customer can consume or sell power to another entity apart from the utility grid; on the contrary in the latter type, end-user can consume and share power only with the utility grid. As more distributed energy resources are connected to the end-user the necessity for optimal management of distributed resources and a framework for reliable operation of these micro grids with the utility grid is becoming increasingly more important.

B. Overview of the Micro Grid Economic Dispatch

Consider an end-user driven micro grid shown in Fig. 1 which includes a PV farm, local load and a battery energy storage connected to the grid. Let P_2 represents the total power which is the algebraic sum of the PV plus the battery. The objective of the economic dispatch is to minimize the cost of the power from the grid at the point of common coupling (PCC) in this case P_2, and at the same time, dispatch the battery for optimal micro grid scheduling. The optimization problem is formulated for a full day operation of the micro grid. The micro grid economic dispatch has a dynamic formulation due to the presence of energy storage which is a time dependent constraint with power and energy limits. This dynamic optimization problem thus provides the dispatch solution at every time stage dependent on the solution of all other time stages. For example in a dynamic economic dispatch for a daily operation, the dispatch solution at noon will depend on the state of the system at that instant and also the past states of the system. In static economic dispatch, the dispatch solutions in a particular time stage only depend on the criteria of that time stage and are independent from the dispatch solutions at other time stages.

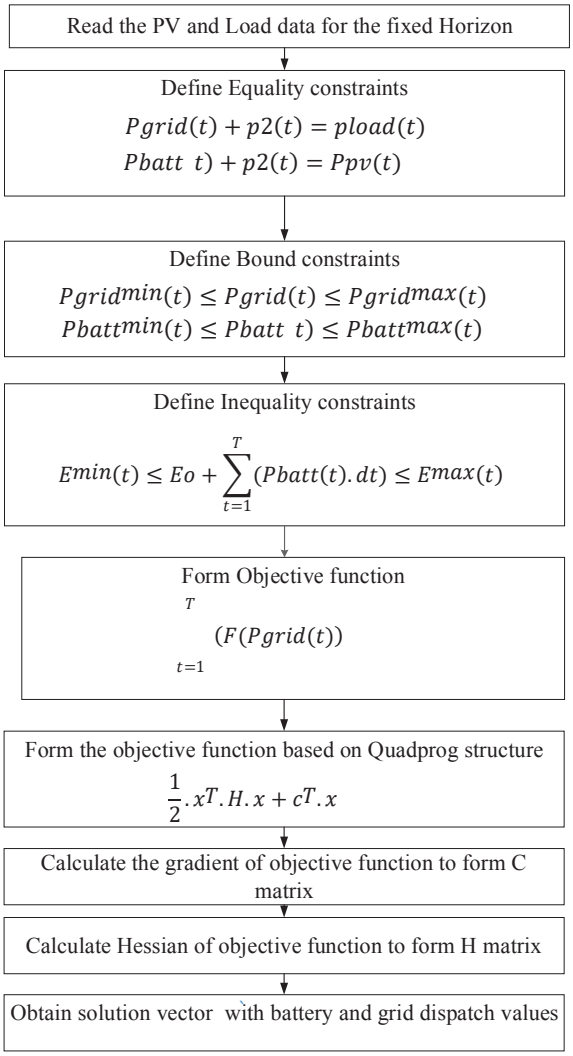

Fig. 2. Flow chart of dynamic optimization algorithm.

C. Proposed Dynamic Economic Dispatch

For the proposed dynamic economic dispatch, a quadratic programming based approach is used to optimize grid cost, which is considered quadratic with linear constraints. Details of a quadratic programming approach is as shown in Fig. 2.

$$\frac{1}{2} \cdot x^T \cdot H \cdot x + C^T \cdot x \tag{1}$$

$$A \cdot x \le b \tag{2}$$

$$A_{eq} \cdot x \le b_{eq} \tag{3}$$

$$l \le x \le u \tag{4}$$

Subsection D discusses the formulation of the objective function and constraints, subsection E discusses modification of the formulation to enable a predictive horizon approach and subsection F illustrates the implementation procedure.

D. Formulation of Objective Function and Constraints for the Proposed Approach

Based on (1)−(4), an objective function, as shown in (5), is proposed for dynamic optimization. It includes the cost function for the grid and battery and other sources available in

the micro grid. Considering a quadratic and convex function, the overall formulation can be represented as

$$\sum_{t=1}^{T}[F(P_{grid}(t))] \tag{5}$$

$$P_{grid}(t) + P_2(t) = P_{load}(t) \tag{6}$$

$$P_2(t) + P_{batt}(t) = P_{pv}(t) \tag{7}$$

$${P_{grid}}^{min}(t) \leq P_{grid}(t) \leq {P_{grid}}^{max}(t) \tag{8}$$

$${P_2}^{min}(t) \leq P_2(t) \leq {P_2}^{max}(t) \tag{9}$$

$${P_{batt}}^{min}(t) \leq P_{batt}(t) \leq {P_{batt}}^{max}(t) \tag{10}$$

$$E^{min}(t) \leq E_0 + \sum_{t=1}^{N} P_{batt}(t) \cdot dt \leq E^{max}(t) \tag{11}$$

where T is the time horizon of the optimization problem and N is the total number of samples.

It is worth noting that the PV and battery operating costs are not incorporated here. This is due to the fact that as a rate pay incentive case, the end-user battery cost is considered always lower than the grid power and thus the cost is insignificant. This is proven in the simulation section. The battery is modeled with minimum and maximum charging and discharging limits. The constraints are formulated such that the load demand is to be met by the PV farm output. The economic dispatch problem is to determine the optimum dispatch of the battery at any given time that minimizes the cost while satisfying the demand and operating limits. $P_{grid}(t)$, $P_2(t)$, $P_{batt}(t)$ are the control variables representing power flows from the grid, PV and battery to the load, respectively, at any given time. Equation (6) implies that the total power supplied by the PV and battery plus the grid must be equal to the load. The constraint in (7) implies that the sum of the battery charging or discharging power and the power supplied directly to the load from the PV is equal to the PV output at that time. During the period of low PV power generation, based on (6), $P_2(t)$ is increased to match the bus load and $P_{grid}(t)$ is decreased. However, as the PV generation is low, the $P_{batt}(t)$ is decreased inheriting a negative sign to satisfy (7). As the PV generation increases and if excess generation is available after satisfying the load, then $P_{batt}(t)$ is increased to satisfy (7), and hence, the battery charges. All the other dispatch variables are constrained by minimum and maximum values as specified by (8)−(11). The algorithmic flow chart is represented in Fig. 2.

1) Formation of the Bounded Constraints: Let us consider the bounded constraints as shown in (12)−(14). The lower bound and upper bound vectors are represented as shown and then concatenated to form the vectors as required. Here N denotes the total number of samples or time scale considered. Since the solution vector consists of three variables the size becomes $3N$.

$$\underset{N\times1}{\left[{P_{grid}}^{min}\right]} \leq \underset{N\times1}{\left[P_{grid}(t)\right]} \leq \underset{N\times1}{\left[{P_{grid}}^{max}\right]} \tag{12}$$

$$\underset{N\times1}{\left[{P_2}^{min}\right]} \leq \underset{N\times1}{\left[P_2(t)\right]} \leq \underset{N\times1}{\left[{P_2}^{max}\right]} \tag{13}$$

$$\underset{N\times1}{\left[{P_{batt}}^{min}\right]} \leq \underset{N\times1}{\left[P_{batt}(t)\right]} \leq \underset{N\times1}{\left[{P_{batt}}^{max}\right]} \tag{14}$$

2) Formation of the Equality Constraints: There are two equality constraints in the above problem as mentioned in (6) and (7). A diagonal identity matrix is considered to implement the above constraint. Such an A_{eq} matrix is formed as shown below in (15)

$$\underbrace{\begin{bmatrix} \begin{bmatrix}1 & \dots & 0\\ \vdots & \ddots & \vdots\\ 0 & \dots & 1\end{bmatrix} & \begin{bmatrix}1 & \dots & 0\\ \vdots & \ddots & \vdots\\ 0 & \dots & 1\end{bmatrix} & \begin{bmatrix}0 & \dots & 0\\ \vdots & \ddots & \vdots\\ 0 & \dots & 0\end{bmatrix} \\ \begin{bmatrix}0 & \dots & 0\\ \vdots & \ddots & \vdots\\ 0 & \dots & 0\end{bmatrix} & \begin{bmatrix}1 & \dots & 0\\ \vdots & \ddots & \vdots\\ 0 & \dots & 1\end{bmatrix} & \begin{bmatrix}1 & \dots & 0\\ \vdots & \ddots & \vdots\\ 0 & \dots & 1\end{bmatrix} \end{bmatrix}}_{2N\times3N} \tag{15}$$

where the structure of the solution vector x is given by

$$\underbrace{\begin{bmatrix} \underset{N\times1}{\left[P_{grid}(t)\right]} \\ \underset{N\times1}{\left[P_2(t)\right]} \\ \underset{N\times1}{\left[P_{batt}(t)\right]} \end{bmatrix}}_{3N\times1} \tag{16}$$

Similarly, the b_{eq} matrix is formed by

$$\underbrace{\begin{bmatrix} \underset{N\times1}{\left[P_{load}(t)\right]} \\ \underset{N\times1}{\left[P_{pv}(t)\right]} \end{bmatrix}}_{2N\times1} \tag{17}$$

3) Formation of the Inequality Constraints: The inequality constraint in (11) is separated into lower and upper limits. The energy stored in the battery at each instant of time is dependent on the charge stored in the battery at the previous instant of time and the (charge/discharge) $P_{batt}(t)$ solution, so we need to sum the $P_{batt}(t)$ solution of previous instants of time. The above constraint can be divided into two inequality constraints. Upper limit of inequality can be written as

$$\sum_{t=1}^{N}(P_{batt}(t) * dt) \leq E^{max} - E_0 \tag{18}$$

where the A matrix as shown in (2) is formed by concatenating matrices (19) and (24).

$$\underbrace{\begin{bmatrix} \underset{N\times N}{\begin{bmatrix}0 & \dots & 0\\ \vdots & \ddots & \vdots\\ 0 & \dots & 0\end{bmatrix}} & \underset{N\times N}{\begin{bmatrix}0 & \dots & 0\\ \vdots & \ddots & \vdots\\ 0 & \dots & 0\end{bmatrix}} & \underset{N\times N}{\begin{bmatrix}1*dt & \dots & 0\\ \vdots & \ddots & \vdots\\ 1*dt & \dots & 1*dt\end{bmatrix}} \end{bmatrix}}_{N\times3N} \tag{19}$$

The b_1 matrix is formed as shown below

$$\underset{N\times1}{\left[E_{max} - E_0\right]} \tag{20}$$

Lower limit of inequality can be written as

$$E^{min} \leq E_0 + \sum_{t=1}^{N}(P_{batt} \cdot dt) \tag{21}$$

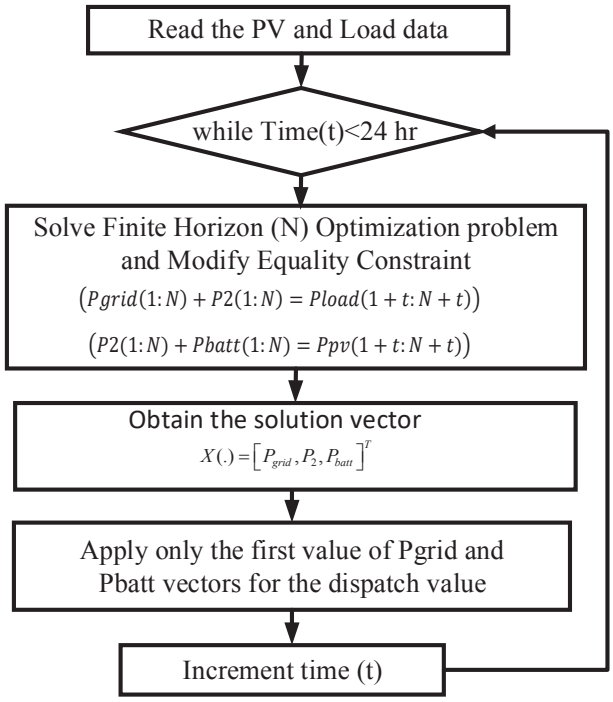

Fig. 3. Flow chart for predictive horizon based optimization.

By converting the above equation into a standard form, we get

$$E^{min} - E_0 \leq \sum_{t=1}^{N} (P_{batt} \cdot dt) \tag{22}$$

$$-E^{min} + E_0 \leq -\sum_{t=1}^{N} (P_{batt} \cdot dt) \tag{23}$$

The A_2 and b_2 matrices are formed as shown below.

$$\underbrace{\left[\begin{bmatrix} 0 & \dots & 0 \\ \vdots & \ddots & \vdots \\ 0 & \dots & 0 \end{bmatrix}_{N\times N} \begin{bmatrix} 0 & \dots & 0 \\ \vdots & \ddots & \vdots \\ 0 & \dots & 0 \end{bmatrix}_{N\times N} \begin{bmatrix} -1*dt & \dots & 0 \\ \vdots & \ddots & \vdots \\ -1*dt & \dots & -1*dt \end{bmatrix}_{N\times N}\right]}_{N\times 3N} \tag{24}$$

$$\underset{N\times 1}{\left[E_0 - E_{min}\right]} \tag{25}$$

Concatenating the b_1 and b_2 matrices to form the b matrix as shown in (2).

$$A = \underset{2N\times 3N}{\begin{bmatrix} A1 \\ A2 \end{bmatrix}}, b = \underset{2N\times 1}{\begin{bmatrix} b1 \\ b2 \end{bmatrix}} \tag{26}$$

E. Predictive Horizon Based Optimization

To illustrate the effect of moving time horizon, a predictive horizon based optimization is designed that modifies the optimization discussed in the previous section. The concept is based on receding horizon control [33], [27], and [34]. Fixed horizon optimization leads to a dispatch schedule, which begins at the current time and ends at some future time. Thus it does not have information regarding the future PV generation and thus the optimal value is not dynamically proven to be optimized. In the predictive horizon approach, PV generation is used for a moving horizon ensuring cost reduction of power from the grid over that horizon. Fig. 3 shows the algorithm

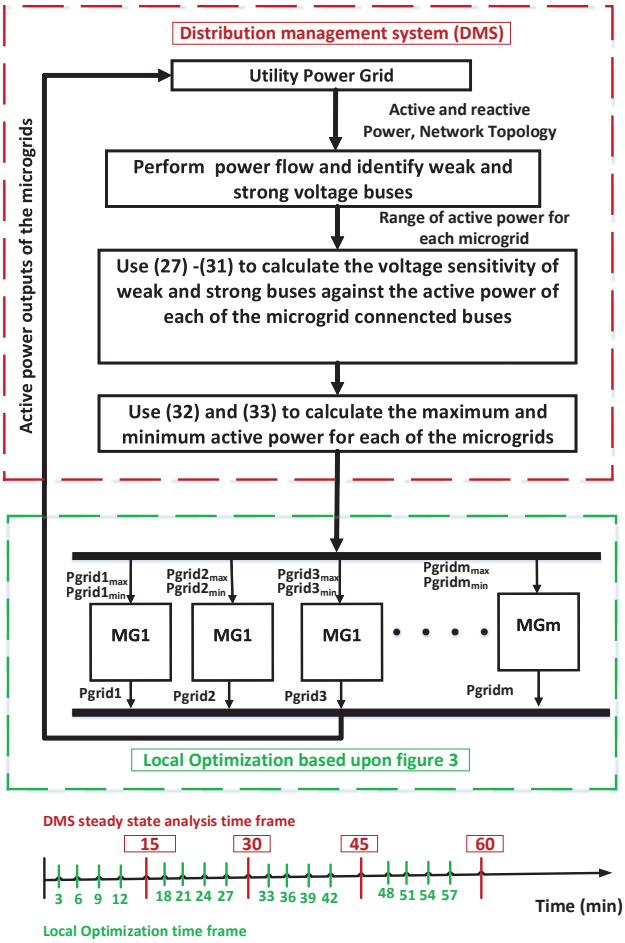

Fig. 4. Proposed overall architecture for operation of end-users driven micro grids with utility power grid.

for predictive horizon based optimization for a day (24 hrs). In this method, dynamic optimization is performed at each time step and only the first value of the optimization is used in the current step. For next time step, the window is moved in time and optimization is performed again. In other words, this method constantly looks for a time horizon in near future and can adjust according to the forecast errors due to passing of clouds or other uncertainties. It can be seen that the proposed approach can provide load schedule set by the end-user (flexibility) and the approach maximizes the local energy resource usage.

F. Framework for Operation With Utility Power Grid

In order to apply the proposed method to a grid connected end-user driven micro grid, security constraints of the interconnected grid needs to be considered. Previous section discuss how the local optimization is performed considering end-user flexibility and local economic benefits. To enable grid level reliability and stability, it has to be made sure that the active power imported or exported to the utility from the micro grid satisfies the voltage security constraints of the grid. To ensure that this condition is satisfied, a framework is proposed that demonstrates the reliable operation of the utility grid with the local optimization of end-user driven micro grids. Fig. 4 illustrates the proposed framework for integrated grid operation.

In this approach, first, steady state analysis (e.g., power flow) is performed at the utility grid to find out the weak and strong voltage buses in the network. Then, using the Jacobian matrix voltage sensitivities of the weak and strong voltage bus is calculated with respect to the active power of micro grid connected buses. Equations (27)−(31) calculate the sensitivities of weak and strong buses. Then using (32)−(33) the maximum and minimum active power range for each of the micro grid connected bus is calculated. If the active power from or to the micro grids exceeds these threshold values then the voltage constraints in the utility grid is violated. The maximum and minimum active power flow obtained after this analysis is then passed to the micro grids as set points. This is then used as a constraint in the local optimization formulation of micro grid as explained in 3. This ensures that although the micro grids are economically dispatched to benefit the end users, it also keeps the active power flow within the designated range for reliable operation of the utility grid. Please note that power flow is generally performed by all utilities as a part of Distributed Management System (DMS) function every 15 to 30 min. This closed loop integration thus allows grid reliability and at the same time provide scheduling capability for the grid based on grid level applications.

$$\begin{bmatrix}\Delta\mathbf{P}\\ \Delta\mathbf{Q}\end{bmatrix} = \begin{bmatrix}\mathbf{J}_{P\theta} & \mathbf{J}_{PV}\\ \mathbf{J}_{Q\theta} & \mathbf{J}_{QV}\end{bmatrix}\begin{bmatrix}\Delta\theta\\ \Delta\mathbf{V}\end{bmatrix} \tag{27}$$

$$\Delta\mathbf{V} = {J_R}^{-1}\cdot\Delta\mathbf{P} \tag{28}$$

$$\mathbf{J}_R = [\mathbf{J}_{PV} - \mathbf{J}_{P\theta}\mathbf{J}_{Q\theta}^{-1}\mathbf{J}_{QV}] \tag{29}$$

$$SVweak_j = \frac{\Delta V_{weak}}{\Delta P_j}, j = 1:m \tag{30}$$

$$SVstrong_j = \frac{\Delta V_{strong}}{\Delta P_j}, j = 1:m \tag{31}$$

$$Pmin_j = \frac{1}{SVstrong_j}\cdot(V_{max} - v_j) - P_j, j = 1:m \tag{32}$$

$$Pmax_j = P_j + \frac{1}{SVweak_j}\cdot(V_j - v_{min}), j = 1:m \tag{33}$$

where $\Delta\mathbf{P}$ is the vector active power deviation for the micro grid connected buses, $\Delta\mathbf{Q}$ is the vector reactive power deviation for the micro grid connected buses, m is the total number of buses where micro grid is connected, $SVweak_j$ is the sensitivity of weak bus voltage with respect to the active power of j^{th} micro grid connected bus, $SVstrong_j$ is the sensitivity of strong bus voltage with respect to the active power of j^{th} micro grid connected bus, $Pmax_j$ is the maximum power allowed at the j^{th} micro grid connected bus, and $Pmin_j$ is the minimum power allowed at the j^{th} micro grid connected bus.

III. Simulation Results and Discussion

The illustration of the dynamic optimization and the predictive optimization is first evaluated on a small test system for one micro grid. Then the proposed framework in Fig. 4 is implemented and evaluated on a real-time practical IEEE test system considering multiple end-user driven micro grids.

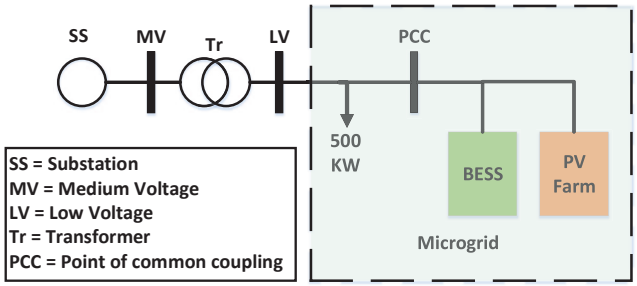

Fig. 5. Proof of concept system representation.

$$N\cdot dt = 24(hr), \quad N\cdot\frac{3}{60} = 24(hr), \quad N = 480 \tag{34}$$

A. Proof of Concept

A small test system as shown in Fig. 5 is used first to demonstrate the effectiveness of the proposed method. For the simulation purpose it is assumed that the micro grid is always connected to the grid. The micro grid devices and its ratings are shown in Table I. The assumed cost function is presented in Table II. The day-ahead forecasted PV power generation utilizing the data acquired from a Southern U.S. location is used for the analysis. Half an hour interval data is read from the data set and the PV generation profile is extracted as shown in Fig. 6. The number of samples obtained from the initial data is based on (34).

TABLE I
Simulation Parameters and Values.

T	24 hr
dt	30 min
BESS	1 MWhr/250 kW
Load	500 kW

TABLE II
Quadratic Cost Coefficients.

Cost function	x^2	x	Constant
Coefficient	0.1	12.6	8

1) Results and Discussions − Fixed Horizon Optimization Considering One Full Day: Fig. 6. shows the dispatch schedule for a full day. During the early morning and night the load is met by the battery and the grid. The battery dispatch is 106 kW during the morning time and 108 kW during evening. As the PV generation increases it produces more power than required by the load. This allows the battery to be charged and also satisfy the load requirement. However, the charging power is optimized such that there is a uniform value of 23 kW power flowing back to the grid so that the overall cost function is minimized. Fig. 7 shows that the SOC has hit the lower limit of 0.2 and also the upper limit of 1 and hence the battery is fully utilized. The cost for the above dispatch schedule was $297.68. Please note that when the SOC is 20 or 100 percent the battery has been considered fully utilized.

2) Results and Discussions − Predictive Horizon: In this approach, the battery schedule is determined considering a one day horizon optimization. For the full day horizon the dispatch set points obtained for the present day also takes the next day PV power profile into consideration. As shown in Table III the cost for $N = 48$ is higher as compared to the cost calculated in fixed horizon optimization which is $297.68.

TABLE III
Cost of RHC With Various Horizon Size

Samples	N=48	N=24	N=12	N=5
Cost($)	309.99	308.95	306.46	278.95

From Fig 8 and Table III, we can observe that as the window size is reduced, the overall cost for predictive horizon based optimization is found to be reduced. For a lower value of window size, the battery discharges more, and hence, the power demanded from the grid is reduced. However, when the window size increases, as it sees the full next-day PV generation schedule, it will give a lower dispatch set point. Even though the cost is higher, the advantage is that the SOC of the battery will be higher at the end of the day. So for the next day the battery power can be used to satisfy the loads and hence grid power required will be reduced. If an opportunity cost is added for the conserved SOC then the overall cost is seen to be lower.

3) Comparison Between Fixed and Predictive Horizon Optimization: To demonstrate the advantage of using the predictive horizon modification both the algorithms were run for three consecutive days considering sunny and cloudy weather days. In fixed horizon case at the end of each day the battery SOC was updated to 100%. If SOC was below a particular value

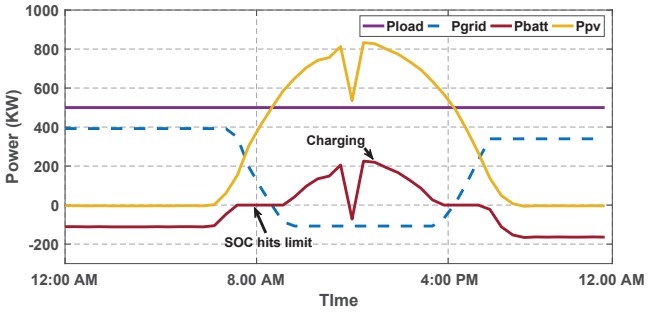

Fig. 6. Simulation results based on dynamic optimization

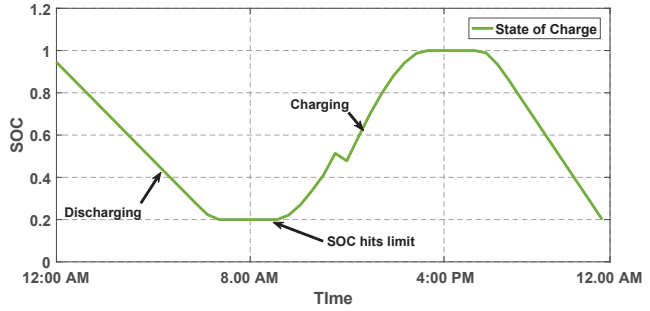

Fig. 7. SOC during optimal dispatch.

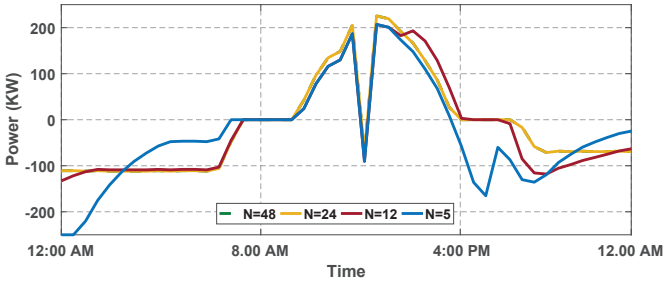

Fig. 8. Predictive horizon battery dispatch for various horizons.

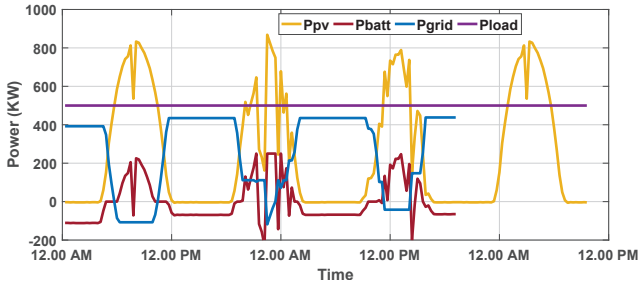

Fig. 9. Predictive horizon 3- day dispatch.

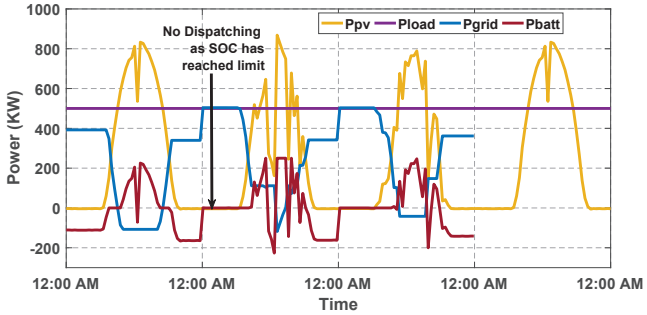

Fig. 10. Fixed horizon 3 day dispatch.

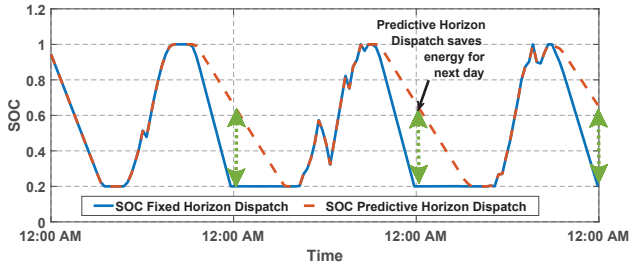

Fig. 11. SOC comparison for predictive and fixed horizon dispatch.

then the cost for the next day was increased by 10% assuming that the grid demand will be higher for the next day. This is done to bring an economic significance to the reduced battery discharge at the end of the day for the predictive horizon optimization dispatch. Fig. 9 and 10 show the comparison of battery dispatch values and the power consumed from grid for predictive horizon and fixed horizon based dispatch. Fig. 11 shows the SOC for both of these dispatch methods.

TABLE IV
Cost of 3 Days Predictive Optimization

Days	Day 1	Day 2	Day 3	Total
Cost($)	309.99	514.70	408.69	1233.38

TABLE V
Cost of 3 Days Fixed Optimization

Days	Day 1	Day 2	Day 3	Total
Cost($)	297.68	566.26	450.29	1314.37

From Fig. 11 it can be seen that the SOC in the case of fixed horizon dispatch has hit the lower limit by midnight of the first day, however, the SOC is about 0.6 (i.e., 60 %) in the predictive optimization case. Hence, the battery can take part in the next day dispatch schedule. This illustrates the fact that the predictive horizon dispatch manages the SOC better than the fixed horizon dispatch which is helpful to tackle future uncertainties in PV power. The net cost was calculated and shown in Tables IV and V. It can be observed from the PV

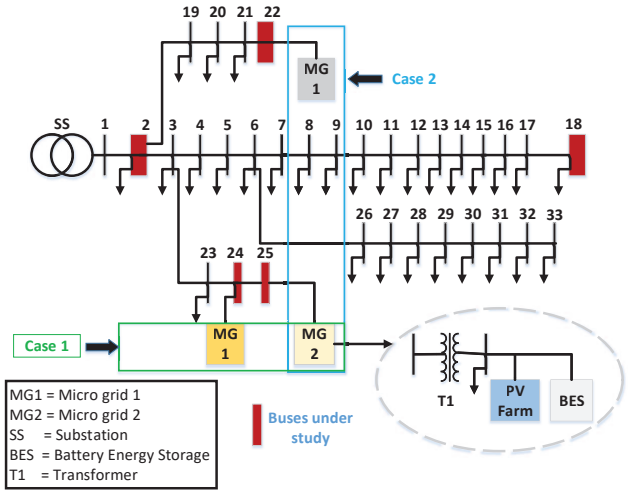

Fig. 12. IEEE 33 bus distribution network.

power profile of Figs. 9 and 10 that Day 1 is sunny, Day 2 is cloudy and Day 3 is partly cloudy. This is also evident from the results of Tables IV and V. Day 1 consumes less grid power and Day 2 consumes more grid power. Moreover, for the first day the fixed horizon optimization gave a lower cost compared to predictive optimization. But for Day-2 since the battery is fully discharged the cost for fixed horizon optimization is higher. Hence considering three consecutive days the total cost is $81 higher for fixed horizon optimization compared to predictive horizon optimization.

B. Application of Proposed Method on a Distribution Feeder

A modified IEEE 33 bus distribution feeder evolved from [35] is used to show the optimized operation of the feeder if there are multiple end-user driven micro grids. A modified schematic diagram of the system including the configuration of the micro grid is shown in Fig. 12. Micro grids can be connected at different buses for different case studies. In this set up, the batteries are considered dispatched according to the economically dispatch values obtained from the optimization

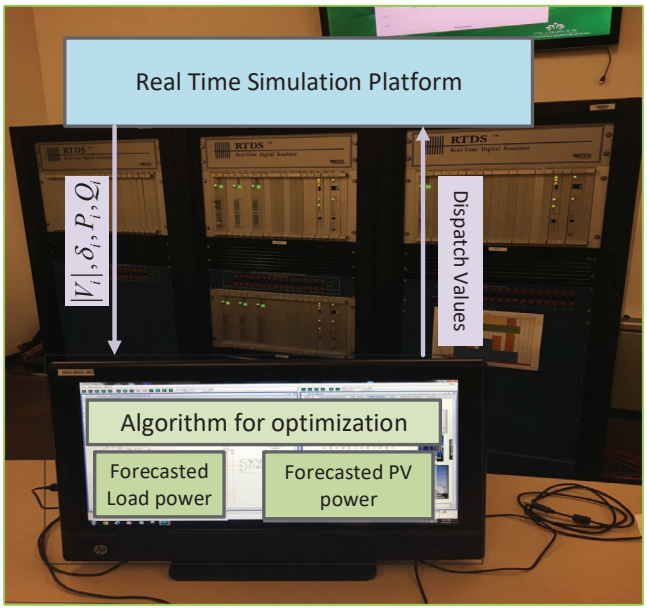

Fig. 13. Experimental setup.

methods mentioned in the previous sections. The voltage profile of the feeder along with the SOC management of the energy storage devices are compared for Receding Horizon Control (RHC) and fixed horizon methods. Voltage profiles of the sensitive buses are marked in red in Fig. 12. Four case studies are performed. Case 1 shows the comparison of the proposed approach with the centralized optimization approach. Case 2 and 3 show the scalability of the proposed approach for multiple micro grids connected in a distribution feeder. In Case 2, two micro grids are located near by and in Case 3 two micro grids are located at different parts of the feeder (see Fig. 12). Case 4 demonstrates the necessity of coordination between local optimization and DMS. Fig. 13 shows the experimental setup for implementing the developed method. A model of the distribution system is illustrated in real-time platform. The algorithm for optimization is implemented in MATLAB 2016b software and run on a separate work station with a CPU clock time of 2.5 Ghz. MATLAB function "quadprog" is used to solve the formulated dynamic optimization problem. It takes on an average of 80 sec to run the optimization for a time horizon of 4 days. Power flow of the system under study is run in Real Time Digital Simulator (RTDS). After obtaining the state variables from the RTDS a static Jacobian based analysis is performed to find the voltage sensitivity of the weak and strong buses. In the system under study, bus 18 is the weak bus and bus 2 is the strong bus. Using the sensitivities values the maximum and minimum power allowed for each of the micro grid buses are calculated. This is then passed to the local optimization of each of the micro grids which generates the dispatch values for the micro grid to follow. Table. VI summarizes the maximum and minimum dispatch values calculated from steady state sensitivity analysis.

TABLE VI
Parameters for Voltage Sensitivity Analysis

Cases	MG	$SVweak_j$	$SVstrong_j$	$Pmax_j$	$Pmin_j$
Case 1	MG1	0.515	0.1	713 kW	-400 kW
Case 1	MG2	0.505	0.094	717 kW	-294 kW
Case 2	MG1	0.495	0.15	722 kW	-433 kW
Case 2	MG2	0.505	0.094	717 kW	-294 kW

1) Case 1: In this case, the results from the proposed approach are compared with a centralized dispatch [16], [20]. We name this as centralized optimization. In the centralized optimization algorithm the power transaction between the grid and micro grid is determined by the centralized dispatch. Then the P_{grid} obtained is used as a net load for the bus where micro grid is connected and an optimal power flow is solved. Fig. 14 shows the comparison of grid power, battery power and the state of charge of battery for both the approaches for fixed load and Fig. 15 shows the comparison for varying load. It can be seen that the centralized optimization approach requires more power to be consumed from the grid compared to the proposed optimization algorithm. Also, large battery idle period can be seen in the case of centralized optimization. Tables VII and VIII further quantify the cost of grid power and shows that the proposed approach saves more compared to the conventional centralized approach for both fixed and varying load. For the varying load condition total kWh of the battery with the proposed approach is 780 kWh for 3 days

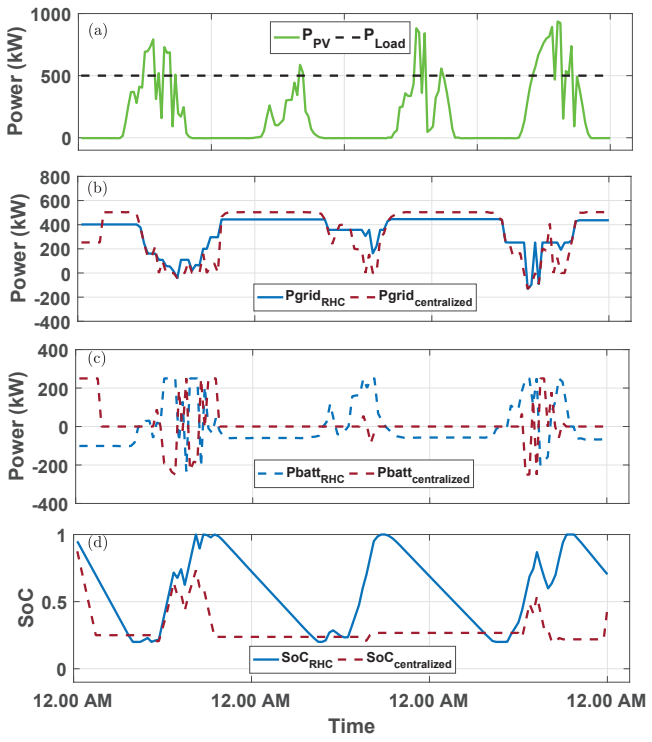

Fig. 14. Case 1: Comparison of proposed approach and centralized approach for fixed load a) PV power and load power b) grid power, c) battery power and d) state of charge of battery.

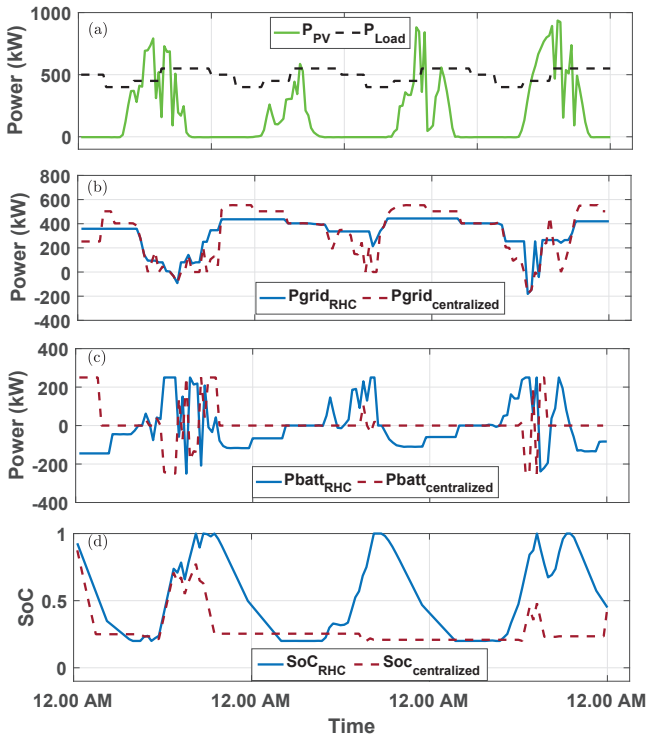

Fig. 15. Case 1: Comparison of proposed approach and centralized approach for varying load a) PV power and load power b) grid power, c) battery power and d) state of charge of battery.

and with the centralized approach the battery output power is 550 kWh. This shows that the proposed approach can use the battery more efficiently.

2) Case 2: In this case, as mentioned, two micro grids MG1 and MG2 are connected to two adjacent buses of the feeder,

TABLE VII
Cost Comparison Between Proposed and Centralized Approach With Fixed Load

Days	Day 1	Day 2	Day 3	Total
RHC($)	534.25	632.7258	536.7758	1703.8
Centralized($)	546.4786	631.01	539.0671	1716.6

TABLE VIII
Cost Comparison Between Proposed and Centralized Approach With Varying Load

Days	Day 1	Day 2	Day 3	Total
RHC($)	518.4685	623.22	532.2858	1668.7
Centralized($)	518.4685	622.83	533.6113	1674.9

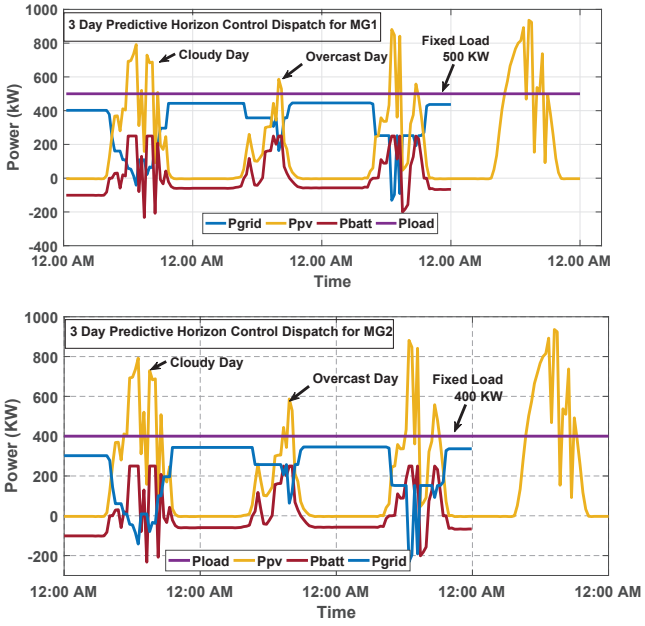

Fig. 16. Case 2: Predictive horizon 3 day dispatch for MG1 and MG2.

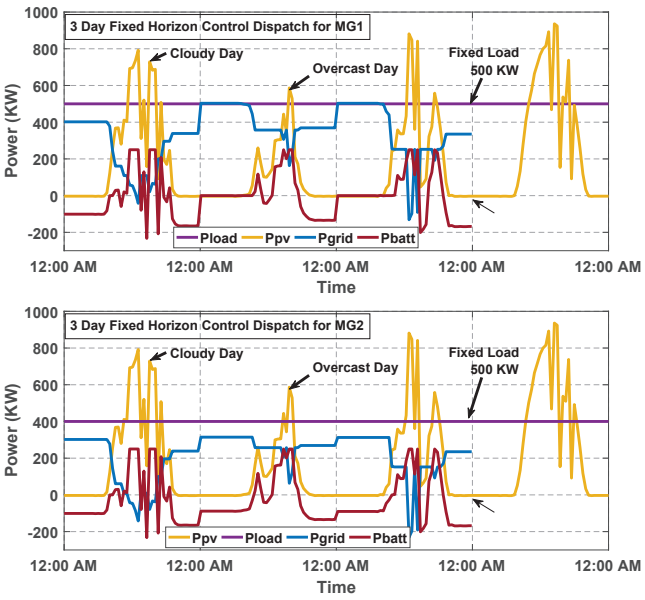

Fig. 17. Case 2: Fixed horizon 3 day dispatch for MG1 and MG2.

i.e., bus 24 and bus 25, respectively. The load at bus 24 and bus 25 is changed to 500 kW from 420 kW and 400 kW from 420 kW, respectively. The PV farm rating and the battery

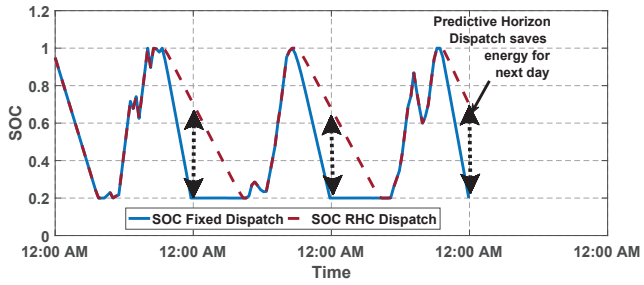

Fig. 18. SOC comparison for predictive and fixed horizon dispatch.

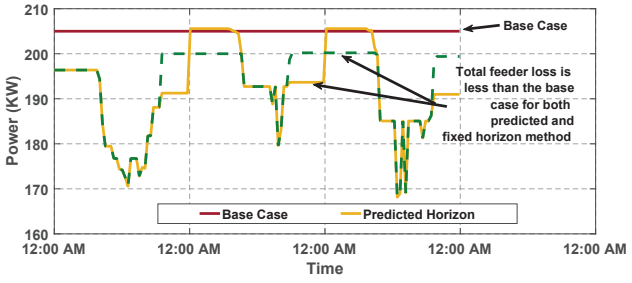

Fig. 19. Case 2: Total active power loss comparison for 3 days.

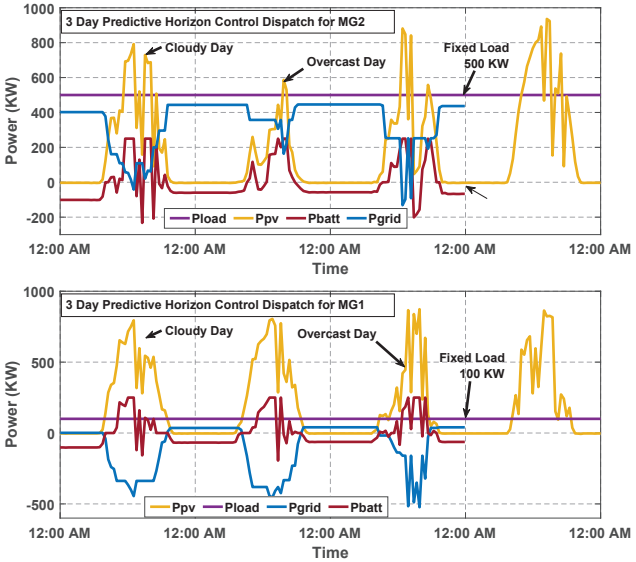

Fig. 20. Case 3: Predictive horizon 3 day dispatch for MG1 and MG2.

configurations are the same for both micro grids. PV power profiles of both PV farms are almost the same as these micro grid buses are considered to be geographically close. One day from each season is randomly chosen for the PV power profile (i.e., total 4 different seasonal days) to demonstrate the application of the proposed method in different seasons.

Figs. 16 and 17 show battery dispatch values, grid power, load power, and PV power for predictive horizon and fixed horizon based dispatch, respectively. Fig. 18 also illustrates the comparison between the SOC for predictive horizon and fixed horizon based optimization method. It shows that predictive horizon method manages the SOC well and SOC is higher compared to the fixed horizon method which is consistent with the results in previous sections. It has been observed that for both predictive horizon and fixed horizon method voltages of all the buses are well within the limit which is 0.9 pu to 1.1 pu for this feeder. The total loss in the active power is also affected

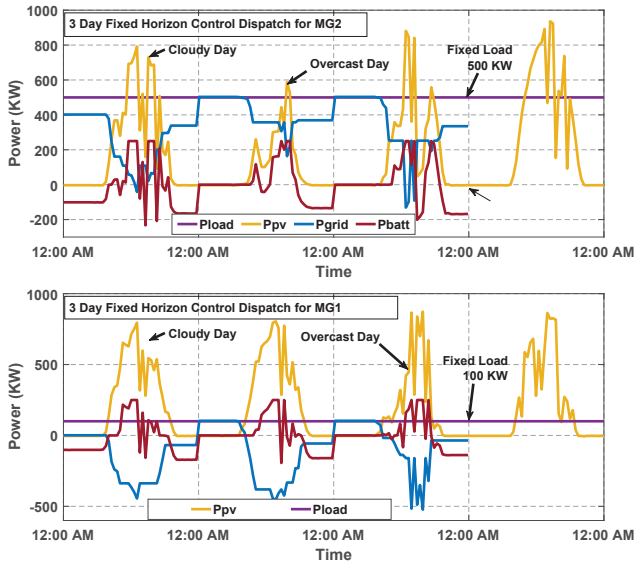

Fig. 21. Case 3: Fixed horizon 3 day dispatch for MG1 and MG2.

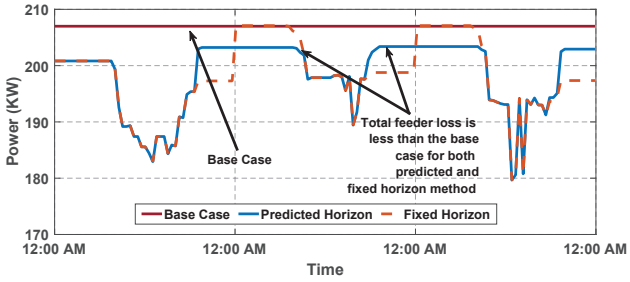

Fig. 22. Case 3: Total active power loss comparison for 3 days.

because of minimizing the power consumed from the grid. From Fig. 19 it can be seen that the active power loss in the feeder is less if battery is dispatched based upon optimization considering cost. For fixed horizon, feeder loss is improved by 6.03% and for predictive horizon, loss is improved by 5.18% compared to the base case where no micro grids are connected. Improvements in voltages are summarized in Table IX.

TABLE IX
Voltage Profile Improvement for Case 2

Bus Number	Bus 2	Bus 22	Bus 25	Bus 18
Predictive Horizon(%)	0.0185	0.3950	0.4879	0.1386
Fixed Horizon(%)	0.0221	0.4710	0.5817	0.1653

3) Case 3: In this case, MG1 is placed at Bus 22 and MG2 is placed at Bus 25. This case is presented to show the effectiveness of the proposed method if the micro grids are not geographically at close proximity. Since two micro grids are located in two different place the PV power profile is considered different for both the PV farms. For analysis purpose, the load at Bus 22 is modified from 90 kW to 100 kW and at Bus 25 load is modified from 420 kW to 500 kW. Figs. 20 and 21 show the optimization results for predictive horizon and fixed horizon dispatch respectively. Fig. 22 illustrates the active power profile comparison. It can be seen that the improvement in losses with fixed horizon and predictive optimization are 4.11% and 4.26%, respectively. The voltage improvements are quantified in Table X.

4) Case 4: This case demonstrates the usefulness of defining maximum and minimum power for each of micro grid

TABLE X
Voltage Profile Improvement for Case 3

Bus Number	Bus 2	Bus 22	Bus 25	Bus 18
Predictive Horizon(%)	0.0164	0.2677	0.2130	0.0704
Fixed Horizon(%)	0.0172	0.2808	0.2267	0.0740

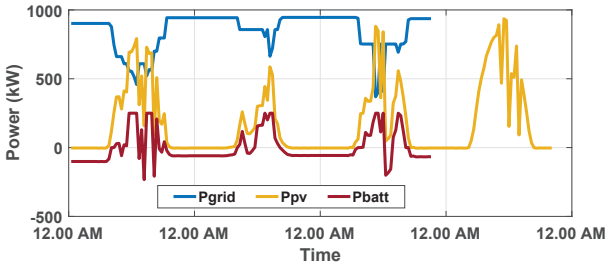

Fig. 23. Case 4: Predictive horizon 3 day dispatch for MG1.

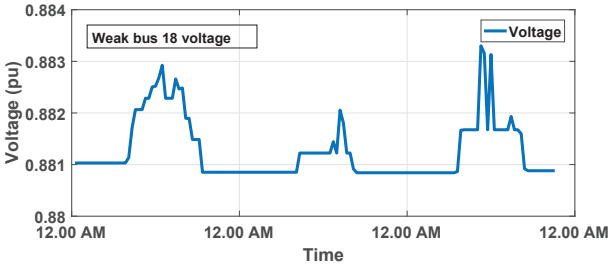

Fig. 24. Case 4: Predictive horizon 3 day dispatch for MG1.

connected bus from the DMS. The experimental set-up for this case is similar to the one in Case 2. In this case no maximum and minimum power limit is enforced on the grid power. It can be seen from Fig. 23 that the active power consumed from the grid for MG1 is greater than the maximum allowed power which is from Table. IV is 713 kW. Fig. 24 illustrates the voltage level of the weakest bus in the feeder which is 18. It can be seen that the voltage goes below the low voltage limit (0.9 p.u) as the power absorbed from the grid by MG1 is more than the maximum power allowed to be consumed from the grid for MG1. So, based upon the steady state analysis in the DMS it is important to always update the maximum and minimum power for each micro grid location.

5) Effect of Battery Cost on The Optimization Result: In this section, the cost function of the battery is added in the objective function of the proposed optimization formulation in (5)− (11). For the cost function of the battery a simple function like a thermal generator is used. The coefficients of the cost function are $a = 0.01$, $b = 3.2$ and $c = 2$. The objective function in (5) is replaced by (35). Then the Case 1 is run again to see the difference in the grid and battery power profile for discarding the battery cost. From Fig. 25 it is observed that there is no noticeable change in the grid and battery power for MG1. Similar affect is seen for MG 2 as well. Similar observations are made for detailed battery cost model as well.

$$\sum_{t=1}^{T}[F(P_{grid}(t)) + F(P_{batt}(t))] \tag{35}$$

6) Overall Analysis: The proposed architecture proves to have the capability to include grid economics, reliability and stability criteria and maximum utilization of the PV and battery

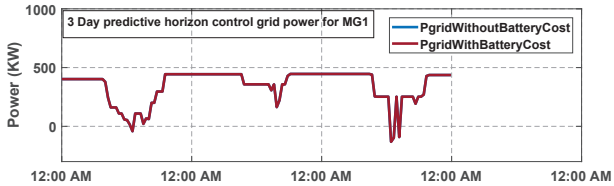

Fig. 25. Comparison of battery dispatch for MG1 with and without battery cost.

system and can be easily integrated with the existing power distribution infrastructure. The method can also be easily modified to accommodate more constraints and scenarios based upon real-time operations. For example, an uncertainty matrix that considers the forecasting errors or change in weather pattern can be included. Also ramp rate constraints for the batteries can be imposed. The approach can also be used to size the battery energy storage more effectively.

IV. Conclusions

In this paper, a new concept of end-user driven micro grid is introduced and an optimal power scheduling approach for the battery dispatch in the micro grid is illustrated. The main contribution of the paper is that unlike other centralized approaches reported in the literature, the proposed architecture provides end-user flexibility, optimally manages the battery minimizing the power required from the grid and at the same time ensures grid level reliability. After evaluating the proof of concept, the proposed optimal scheduling is compared with one of the existing centralized optimization approaches. Furthermore, the scalability of the algorithm on a power distribution feeder is illustrated with two micro grids connected at different points. Test results demonstrated that the proposed approach perform better than the centralized approach in terms of optimal battery scheduling, end-user flexibility, and minimizing the overall cost. Moreover, the real-time implementation showed that the proposed architecture is feasible and scalable, and it also ensure the grid level reliability.

References

[1] J. C. Vasquez, J. M. Guerrero, J. Miret, M. Castilla, and L. G. de Vicuna, "Hierarchical control of intelligent microgrids," *IEEE Industrial Electronics Magazine*, vol. 4, no. 4, pp. 23–29, Dec 2010.

[2] A. G. Tsikalakis and N. D. Hatziargyriou, "Centralized control for optimizing microgrids operation," in *2011 IEEE Power and Energy Society General Meeting*, July 2011, pp. 1–8.

[3] M. T. Burr, M. J. Zimmer, G. Warner, B. Meloy, J. Bertrand, W. Levesque, and J. D. McDonald, "Emerging models for microgrid finance: Driven by the need to deliver value to end users." *IEEE Electrification Magazine*, vol. 2, no. 1, pp. 30–39, March 2014.

[4] S. Suryanarayanan, R. K. Rietz, and J. Mitra, "A framework for energy management in customer-driven microgrids," in *IEEE PES General Meeting*, July 2010, pp. 1–4.

[5] S. Suryanarayanan and J. Mitra, "Enabling technologies for the customer-driven microgrid," in *2009 IEEE Power Energy Society General Meeting*, July 2009, pp. 1–3.

[6] P. Jain, S. J. Ranade, S. Gupta, and E. Pontelli, "Optimum operation of a customer-driven microgrid: A comprehensive approach," in *2012 IEEE International Conference on Power Electronics, Drives and Energy Systems (PEDES)*, Dec 2012, pp. 1–6.

[7] Y. Xiang, J. Liu, and Y. Liu, "Robust energy management of microgrid with uncertain renewable generation and load," *IEEE Transactions on Smart Grid*, vol. 7, no. 2, pp. 1034–1043, March 2016.

[8] H. L. G. Chang and H. Su, "Short-term distributed energy resource scheduling for a dc microgrid," *Energy and Power Engineering*, vol. 5, no. 4B, pp. 15–21, 2013.

[9] A. D. Giorgio, F. Liberati, A. Lanna, A. Pietrabissa, and F. D. Priscoli, "Model predictive control of energy storage systems for power tracking and shaving in distribution grids," *IEEE Transactions on Sustainable Energy*, vol. 8, no. 2, pp. 496–504, April 2017.

[10] A. D. Giorgio, F. Liberati, and A. Lanna, "Real time optimal power flow integrating large scale storage devices and wind generation," in *2015 23rd Mediterranean Conference on Control and Automation (MED)*, June 2015, pp. 480–486.

[11] A. Nottrott, J. Kleissl, and B. Washom, "Storage dispatch optimization for grid-connected combined photovoltaic-battery storage systems," in *2012 IEEE Power and Energy Society General Meeting*, July 2012, pp. 1–7.

[12] Matlab. Interior-point-convex quadprog algorithm. http://www.mathworks.com/help/optim/ug/quadratic-programming-algorithms.html#bsqspm.

[13] P. M. Corrigan and G. T. Heydt, "Optimized dispatch of a residential solar energy system," in *2007 39th North American Power Symposium*, Sept 2007, pp. 183–188.

[14] M. D. Hopkins, A. Pahwa, and T. Easton, "Intelligent dispatch for distributed renewable resources," *IEEE Transactions on Smart Grid*, vol. 3, no. 2, pp. 1047–1054, June 2012.

[15] P. Mahat, J. E. Jimnez, E. R. Moldes, S. I. Haug, I. G. Szczesny, K. E. Pollestad, and L. C. Totu, "A micro-grid battery storage management," in *2013 IEEE Power Energy Society General Meeting*, July 2013, pp. 1–5.

[16] S. Teleke, M. E. Baran, S. Bhattacharya, and A. Q. Huang, "Rule-based control of battery energy storage for dispatching intermittent renewable sources," *IEEE Transactions on Sustainable Energy*, vol. 1, no. 3, pp. 117–124, Oct 2010.

[17] S. Moghadasi and S. Kamalasadan, "Real-time optimal scheduling of smart power distribution systems using integrated receding horizon control and convex conic programming," in *2014 IEEE Industry Application Society Annual Meeting*, Oct 2014, pp. 1–7.

[18] S. Abdelrazek and S. Kamalasadan, "Integrated control of battery energy storage management system considering pv capacity firming and energy time shift applications," in *2014 IEEE Industry Application Society Annual Meeting*, Oct 2014, pp. 1–7.

[19] S. A. Abdelrazek and S. Kamalasadan, "A weather-based optimal storage management algorithm for pv capacity firming," *IEEE Transactions on Industry Applications*, vol. 52, no. 6, pp. 5175–5184, Nov 2016.

[20] Y. Riffonneau, S. Bacha, F. Barruel, and S. Ploix, "Optimal power flow management for grid connected pv systems with batteries," *IEEE Transactions on Sustainable Energy*, vol. 2, no. 3, pp. 309–320, July 2011.

[21] J. Z. H. Tazvinga, X. Xia, "Minimum cost solution of photovoltaic-diesel-battery hybrid power systems for remote consumers," *Solar Energy*, vol. 96, pp. 292–299, 2013.

[22] K. Baker, J. Guo, G. Hug, and X. Li, "Distributed mpc for efficient coordination of storage and renewable energy sources across control areas," *IEEE Transactions on Smart Grid*, vol. 7, no. 2, pp. 992–1001, March 2016.

[23] . Ortega, P. M. Namara, and F. Milano, "Design of mpc-based controller for a generalized energy storage system model," in *2016 IEEE Power and Energy Society General Meeting (PESGM)*, July 2016, pp. 1–5.

[24] C. Eksin, A. Hooshmand, and R. Sharma, "A decentralized energy management system," in *2015 European Control Conference (ECC)*, July 2015, pp. 2260–2267.

[25] M. Mahmoodi, P. Shamsi, and B. Fahimi, "Economic dispatch of a hybrid microgrid with distributed energy storage," *IEEE Transactions on Smart Grid*, vol. 6, no. 6, pp. 2607–2614, Nov 2015.

[26] T. Paul, S. Ghosh, S. Kamalasadan, and P. Mandal, "A quadratic programming based optimal power and battery dispatch for grid connected microgrid," in *2016 IEEE Industry Applications Society Annual Meeting*, Oct 2016, pp. 1–8.

[27] B. Lu and M. Shahidehpour, "Short-term scheduling of battery in a grid-connected pv/battery system," *IEEE Transactions on Power Systems*, vol. 20, no. 2, pp. 1053–1061, May 2005.

[28] S. J. Chiang, K. T. Chang, and C. Y. Yen, "Residential photovoltaic energy storage system," *IEEE Transactions on Industrial Electronics*, vol. 45, no. 3, pp. 385–394, Jun 1998.

[29] C. Wang and M. H. Nehrir, "Power management of a stand-alone wind/photovoltaic/fuel cell energy system," *IEEE Transactions on Energy Conversion*, vol. 23, no. 3, pp. 957–967, Sept 2008.

[30] S. Jain and V. Agarwal, "An integrated hybrid power supply for distributed generation applications fed by nonconventional energy sources," *IEEE Transactions on Energy Conversion*, vol. 23, no. 2, pp. 622–631, June 2008.

[31] N. H. E.-F. Xiaonan Wang, Ahmet Palazoglu, "Operational optimization and demand response of hybrid renewable energy systems," *Elsevier Applied Energy*, vol. 143, pp. 324–335, 2015.

[32] H. Kanchev, D. Lu, F. Colas, V. Lazarov, and B. Francois, "Energy management and operational planning of a microgrid with a pv-based active generator for smart grid applications," *IEEE Transactions on Industrial Electronics*, vol. 58, no. 10, pp. 4583–4592, Oct 2011.

[33] L. Xiaoping, D. Ming, H. Jianghong, H. Pingping, and P. Yali, "Dynamic economic dispatch for microgrids including battery energy storage," in *The 2nd International Symposium on Power Electronics for Distributed Generation Systems*, June 2010, pp. 914–917.

[34] J. Mattingley, Y. Wang, and S. Boyd, "Code generation for receding horizon control," in *2010 IEEE International Symposium on Computer-Aided Control System Design*, Sept 2010, pp. 985–992.

[35] M. E. Baran and F. F. Wu, "Network reconfiguration in distribution systems for loss reduction and load balancing," *IEEE Transactions on Power Delivery*, vol. 4, no. 2, pp. 1401–1407, Apr 1989.

T. George Paul (S' 08) received his M.S degree in electrical engineering from the University of North Carolina at Charlotte and B.E degree in electrical engineering from Anna University, India. He joined Schweitzer Engineering Laboratories Engineering Services division in 2016 as a power system engineer focusing on power system modeling using a Real Time Digital Simulator for testing power management schemes. He has experience in the field of power system protection and automation.

S. J. Hossain (S' 16) received the B.Sc in Electrical and Electronic Engineering from Bangladesh University of Engineering and Technology, Bangladesh, in 2013. He worked as a software engineer in Samsung Research and Development institute Bangladesh from 2013 to 2015. He is currently a PhD candidate at University of North Carolina at Charlotte. His research interests are distributed energy systems integration, modeling and control, and wide area monitoring, optimization and control of power system.

S.Ghosh (M' 12) received the B. Tech degree from National Institute of Technology (NIT) Jamshedpur, India, in 2002, the M.Tech degree from NIT Durgapur, Durgapur, India, in 2009, and the Ph.D. degree from Indian Institute of Technology, Delhi, India, in 2013. He is currently a faculty member at UNC Charlotte. Previously, he was an Assistant Professor with the Department of Electrical Engineering, Indian School of Mines, Dhanbad, India. His research interests include the areas of power system small-signal stability, power system modeling and dynamic analysis.

P. Mandal (S05, M06, SM12) received the M.E. and B.E. degrees from Thailand and India, respectively, and the Ph.D. degree from the University of the Ryukyus, Japan, in 2005. He is presently an Associate Professor of Electrical and Computer Engineering at the University of Texas at El Paso, TX, USA. His research interests include power systems operations and markets, power system optimization, renewable energy integration and forecasting.

S. Kamalasadan (SM'01, M'05, SM'17) received his Ph.D. in Electrical Engineering from the University of Toledo, Ohio in 2004, M.Eng in Electrical Power Systems Management, from the Asian Institute of Technology, Bangkok Thailand in 1999 and B Tech. degree in Electrical and Electronics from the University of Calicut, India in 1991. He is currently working as a Professor in the department of electrical and computer engineering at the University of North Carolina at Charlotte.